Surface Shape Change During Fusion of Erythrocyte Membranes Is Sensitive to Membrane Skeleton Agents

Yankuan Wu, Jason D. Rosenberg, and Arthur E. Sowers
Department of Pathology, School of Medicine, University of Maryland, Baltimore, Maryland 21201 USA

ABSTRACT We previously reported that the induction of membrane fusion between pairs of erythrocyte ghosts is accompanied by the formation of a multipore fusion zone that undergoes an area expansion with condition-dependent characteristics. These characteristics allowed us to hypothesize substantial, if not major, involvement of the spectrin-based membrane skeleton in controlling this expansion. It was also found that the fusion zone, which first appears in phase optics as a flat diaphragm, has a lifetime that is also highly condition-dependent. We report here that 2,3-diphosphoglycerate, wheat germ agglutinin, diamide, and *N*-ethylmaleimide, all known to have binding sites primarily on skeleton components (including spectrin), have condition-dependent effects on specific components of the fusion zone diameter versus time expansion curve and the flat diaphragm lifetime. We also report a pH/ionic strength condition that causes a dramatic stabilization of flat diaphragms in a manner consistent with the known pH/ionic strength dependence of the spectrin calorimetric transition, thus further supporting the hypothesis of spectrin involvement. Our data suggest that the influence of the membrane skeleton on cell fusion is to restrain the rounding up that takes place after membrane fusion and that it may have variable, rather than fixed, mechanical properties. Data show that WGA, a known ligand for sialic acid, and DPG, a known metabolite, influences the flat diaphragm stability and late period expansion rates, raising the possibility that some of these mechanical properties are biologically regulated.

INTRODUCTION

The results reported in this paper deal with the relationships between the mechanical function of the spectrin-based membrane skeleton in plasma membranes, the rounding-up process that occurs when two cells fuse with each other, and the stability of two close spaced membranes when they contain numerous fusion pores (i.e., a membrane fusion zone).

The spectrin-based membrane skeleton, a protein network understood to be a part of the cytoplasmic surface of plasma membranes of all nucleated cells, is relatively well characterized in terms of the *structure* of its major components in erythrocytes (for review, see Bennett, 1990). Electron microscopy studies show isolated spectrin (Branton et al., 1981) as a rod-like molecule and the native skeleton as an assembly of components, which is in the form of a complex but essentially two dimensional array (Byers and Branton, 1985; McGough and Josephs, 1990; Ursitti and Wade, 1993). Much less well understood, however, are erythrocyte skeleton-related *functions* and the molecular mechanisms by which these functions are *regulated*. In general, the skeleton is widely understood to provide the membrane with strength and deformability while preserving integrity, a means for controlling shape and shape change, and a physical framework with anchor points for other cytoskeletal elements and membrane components. Also, many protein deficiencies or defective interactions among membrane skeleton components have been identified that lead to altered properties that ultimately become expressed as disease states (Palek and Lux, 1983). Interdisciplinary studies using an approach that combines mathematical modeling and the micropipette technique have permitted measures of both fundamental (dimension-based) mechanical properties and relative (dimensionless) mechanical factors (Evans, 1989). Further studies using this approach have permitted correlations to be made between membrane skeleton components responsible for specific fundamental mechanical properties and general physiological functions (Waugh and Agre, 1988). In addition, physical modeling (for a review, see Elgsaeter et al., 1986) and the bilayer couple hypothesis (Sheetz and Singer, 1974) have been used to explain the control of cell shape. However, the control of shape by other factors as induced either under physiologically relevant (for reviews, see Bessis, 1973; Beaudoin and Grondin, 1991) or xenobiological conditions (for reviews, see Lew et al., 1988; Deuticke, 1968) is still poorly understood.

Cell fusion is a widely occurring and essential process by which two cells become one cell. Although this process occurs in nature with many well recognized system-specific details, it is also associated with both subtle and not widely appreciated caveats as well as unsolved problems. In cell culture studies of enveloped virus-cell interactions, for example, cell fusion occurs when numerous individual cells become part of a syncytium, a multinuclear cytoplasmic mass that either stays spread out and attached to the substrate or undergoes a process in which the fusing cells round up into a sphere (Roizman, 1962). The scenario in which two small spherical cells combine into one larger spherical fusion product is known to occur in model systems such as chemically induced protoplast fusion (Senda et al., 1979; Boss, 1987) and in various fusions of spherical nucleated mammalian

Received for publication 16 June 1994 and in final form 18 August 1994.
Address reprint requests to Dr. Arthur E. Sowers, Department of Pathology, School of Medicine, University of Maryland, 10 South Pine St., Baltimore, MD 21201. Tel.: 410 706 0720; Fax: 410 706 8414; E-mail: arthures@aol.com.

Dr. Wu's present address: The Upjohn Company, Kalamazoo, MI 49001.

0006-3495/94/11/1896/10 $2.00

cells as induced by, for example, laser light pulses (Schierenberg, 1987; Steubing et al., 1991), chemicals (Lucy, 1978), and enveloped viruses (Knutton, 1977; Sarkar et al., 1989). Because surface (interfacial) tension is known to drive the rounding up of cell fragments (Harvey, 1954), the whole cell fusion process appears to take place in a manner that suggests that it is self-completing, passive, and otherwise essentially unremarkable. Understandably, as investigators gradually recognized that membrane fusion was a necessary condition for cell fusion and that membrane fusion could be investigated with molecular or near-molecular level paradigms, interest shifted from primarily descriptive studies (often in connection with genetic experiments) at the *cell* level (e.g., Harris, 1970; Ringertz and Savage, 1976) to what happens at the *membrane* level (Poste and Nicolson, 1978; White, 1992; Duzgunes, 1993a, b). The observation that membrane fusion can occur under conditions in vitro without the subsequent rounding up (cell fusion) (Wojcieszyn et al., 1983) means, however, that membrane fusion is necessary but not sufficient for cell fusion and is relevant to two fundamental questions. First, how *independent* can cell fusion be from membrane fusion? And second, is the rounding up process in any way under biological *control*? For virus-induced cell fusion systems (see, e.g., Sarkar et al., 1989), fusion zones containing multiple fusion pores have to break down for rounding up to become complete, but the factors involved are not well understood. For secretion systems, fusion zones contain only one fusion pore. In these systems, some parameters and conditions for single fusion pore induction, stability, and expansion in diameter have been elucidated (Monck et al., 1990, 1991; Oberhauser et al., 1992). These questions are directly relevant to virus-cell interactions where syncytium formation is a significant observable parameter. Some studies suggest that this process is influenced by biological factors (see, e.g., Grimalla et al., 1992; Horvath et al., 1992), although the detailed mechanisms by which this takes place are clearly not well understood.

Recently, we have found (Chernomordik and Sowers, 1991) that the induction of fusion in erythrocyte ghosts by an electric pulse starts with the conversion of a contact zone into a membrane fusion zone that appears in phase optics microscopy as a flat, optically dense "diaphragm" at ghost-ghost junctions (Figs. 1 and 2). In electron microscopy the flat diaphragm appears as a double membrane perforated with multiple fusion pores (see Fig. 1, *left inset*). This ultrastructure is identical to that induced by enveloped viruses (Knutton, 1977; Pinto da Silva et al., 1980). Furthermore, the electrofused erythrocyte ghosts round up over a time scale that is similar to the fusion-related rounding up seen in many other cell fusion systems (see Discussion). We subsequently found (Wu et al., 1994) that the "flat diaphragm" has a condition-dependent *lifetime*; the flat diaphragm can be stable for at least many days or be unstable and quickly break down into membrane fragments, thus leaving the fusion zone as an "open lumen." Moreover, the fusion zone diameter expands with time also in a condition-dependent manner, concomitantly with the rounding up of the fusion product. Finally, the manner in which the fusion zone diameter expansion "signature" was sensitive to heat treatments (and protected by glycerol) suggested that spectrin and/or the membrane skeleton was involved in the rounding up process.

We report here that the fusion zone diameter versus time expansion curve and the flat diaphragm lifetime are altered in condition-dependent but different ways by 2,3-diphosphoglycerate (also known as 2,3-bisphosphoglycerate), wheat germ agglutinin, diamide, and *N*-ethylmaleimide. We also report a pH/ionic strength condition that causes a dramatic stabilization of flat diaphragms in a manner consistent with the known pH/ionic strength dependence of the spectrin calorimetric transition, thus further supporting the hypothesis of spectrin involvement. Because these chemical species are all known to have binding sites on skeleton components (including spectrin) and also to have influences on erythrocyte deformability and stability (see Discussion), our data suggest that the influence of the membrane skeleton on cell fusion is substantial and that it may act as an entity with variable, rather than fixed, mechanical properties. The effects of WGA and DPG suggest at least the potential for some of these mechanical properties to be biologically regulated. Our data, together with data published from other laboratories, suggest that the membrane skeleton *restrains* the rounding up that takes place after membrane fusion. Our experimental approach, which uses fused pairs of erythrocyte ghosts, allows latent membrane-skeleton forces to be released under conditions in which the membrane skeleton is at least relatively intact. This approach may be useful in broader studies because it permits the study of hitherto uncharacterized relationships between experimental conditions and the mechanical properties of the membrane skeleton as well as the stability of multiple pore fusion zones.

MATERIALS AND METHODS

Overview-approach

This study utilized the electrofusion protocol (Sowers, 1993) to fuse pairs of erythrocyte ghosts (Figs. 1 and 2) and to fuse mitochondrial inner membranes (Sowers, 1983). The erythrocyte ghost membrane has a membrane skeleton but is essentially free of other cytoplasmic elements that are normally found in nucleated cells. The mitochondrial inner membrane, as prepared here, contains a diluted complement of soluble matrix proteins and mitochondrial DNA, but is otherwise a biomembrane having no recognized membrane skeleton. The electric pulse method (Sowers, 1993) of inducing membrane fusion was used to avoid significant and multiple complicating effects that could be expected from the presence of chemical or biological fusogens and to take advantage of its ability to produce, at will, high yields and simultaneity (<100 ms (Abidor and Sowers, 1992)) of membrane fusion events. Membranes were brought into contact (a prerequisite for any membrane fusion protocol) by dielectrophoretic alignment (Pohl, 1978) into pearl chains by passing a weak alternating electric current through the membrane suspension. Use of this mild, reversible, and nonchemical method together with the electric pulse, as a fusogen, permits membrane-membrane contact, membrane fusion, membrane type, and buffer composition to be manipulated independently. Most of the experiments in the present study were conducted with heat treatments at a temperature of either 39 or 42°C before the fusion zone measurements because use of these temperatures was found (Chernomordik and Sowers, 1991; Wu et al., 1994) to lead to early flat

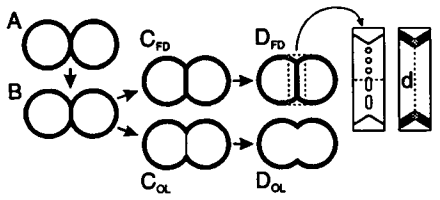

FIGURE 1 Electrofusion of a pair of erythrocyte ghosts as it appears in phase optics. Dielectrophoresis induces close membrane-membrane contact at a contact zone (*A*). An electric pulse induces fusion pores in the contact zone, thus converting it into a flat diaphragm fusion zone, visible as a short but thick optically dense straight line (*B*). This line increases in length (C_{FD}) with time and is still visible at the end (D_{FD}) of the observation period. The flat diaphragm appears to "dissolve" (C_{OL}) by becoming thinner and longer if the ghosts are exposed to a 20 min heat treatment at 42°C, or above, before the induction of membrane fusion. This thinning process ends with the fusion zone having an "open lumen" appearance (D_{OL}). The left inset illustrates how the flat diaphragm appears by electron microscopy (cf. Fig. 4 in Chernomordik and Sowers, 1991) when it has a high (*upper half*) or low (*lower half*) fusion site density. The right inset illustrates where cursors were placed on the monitor image of the fusion zone to make diameter measurements. The thicknesses of the lines used in each inset are approximately in proportion to what is actually seen by the two microscopy techniques.

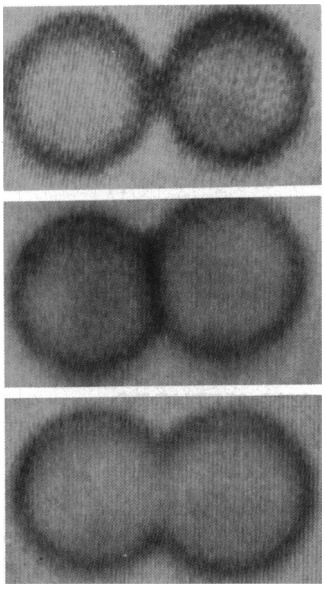

FIGURE 2 Micrographs of a phase optics video image of a pair of erythrocyte ghosts held in contact by dielectrophoresis (*top*), a flat diaphragm fusion zone with a diameter of ~3.5 μm (*middle*), and an open lumen fusion zone with approximately the same diameter (*bottom*) but produced from fusion of a different pair of erythrocyte ghosts.

diaphragm breakdown, an observable that is easy to score, as well as a higher rate of fusion zone expansion that could be measured more accurately than a lower rate.

Preparation of erythrocyte membranes

Unless otherwise specified, rabbit erythrocyte ghost membranes were prepared and stored as previously described (Wu et al., 1994). Briefly, this involved washing 0.75–1.0 ml of packed erythrocytes in pH 7.4 isotonic sodium phosphate (NaPi) buffer followed by a hemolysis in 5 mM pH 8.5 NaPi buffer, pelleting into a volume of 0.5–0.75 ml followed by resuspension with 25 ml of 20 mM pH 8.5 NaPi buffer (wash buffer) followed by a resuspension of the membrane pellet with 1.5 ml of the same buffer (resuspension buffer). The membranes in these preparations had morphologies ranging from stomatocytes to spherocytes and produced a pink pellet on centrifugation. Spherocytic and near-spherocytic membranes were preferentially selected for study. The suspensions of these membranes either were used in fusion protocols without further treatments (control) or were subjected to heat and/or chemical treatments as described below before the induction of membrane fusion. Images of the fusion process were recorded on video tape for subsequent playback and quantitative analysis.

Preparation of mitochondrial inner membranes

Mitochondrial inner membranes were prepared and osmotically swollen into smooth spherical forms in a low ionic strength buffer as previously described (Sowers and Hackenbrock, 1981; Sowers, 1983) and used in that buffer, or were centrifuged and resuspended in 20 mM pH 7.4 NaPi for experiments.

Protocol for electrofusing erythrocyte membranes

Membrane suspension samples were stored, unless otherwise stated, at 0–4°C until samples were transferred to the observation chamber (see below), where the temperature was kept at 20–22°C. Pearl chains of erythrocyte ghosts were obtained by inducing dielectrophoretic alignment with an alternating electric field of 3.25 V_{rms}/mm (60 Hz sine wave), over a 1–2 min period, and then electrofused by applying a single exponentially decaying (0.55 ms decay half-time) electric field pulse (600 V/mm) as described in Sowers (1993) and using a chamber described in Abidor and Sowers (1992). In this protocol, the alternating electric field was continuously present at the same strength both before and after the fusogenic pulse. These conditions are known (Sowers, 1993) to induce high (≥60–80%) membrane fusion yields as measured by membrane mixing using lipid-soluble fluorescent labels.

Protocol for electrofusing mitochondrial inner membranes

Suspended mitochondrial inner membranes were placed in the chamber and aligned into pearl chains, containing at least two membrane members, by dielectrophoresis with an alternating electric field of 10–15 V/mm (60 Hz) and fused with a single exponentially decaying (1 ms decay half-time) electric field pulse (1000 V/mm). These fields are stronger than those used to fuse erythrocyte ghosts because it is known that the induction of dielectrophoresis and fusogenic membrane potentials in smaller diameter membranes requires higher external bulk fields (Sowers and Kapoor, 1988; Gross et al., 1986).

Measurements and observations by phase optics microscopy

For data collection only pairs of erythrocyte ghosts were visually selected from a field containing numerous pearl chains. Fusion zone diameters (Fig. 1) for fused pairs of erythrocyte ghosts were measured as a function of time using image analysis software on images captured by a frame-grabber from recorded video sequences containing embedded time data as previously described (Wu et al., 1994). The first diameter measured was at 0.5 s after the pulse. The flat diaphragm lifetime was determined for every fused pair of ghost membranes during single frame or slow playback of recorded video sequences by estimating the midpoint between the time that a given flat diaphragm was perceived to begin to "dissolve" and the time that it was no longer discernable (see Fig. 2). Final fusion zone type (flat diaphragm or open lumen) was determined from evaluation of fusion products at the end (120 s after fusion) of the video sequence. Fusions of mitochondrial inner

membranes were visually observed in real time using a 1.3 numerical aperture oil immersion 100X phase objective (technical factors prevented the recording of publication quality images).

Instrumentation accuracy and characteristics of the phenomenon

The characteristics of the erythrocyte ghost fusion zone expansion and the optical resolution (~1.0–1.5 μm for our 0.55NA LWD 40X phase objective) as well as pixel resolution, reproducibility, and video noise (Σ~0.45 μm) introduce limitations as follows (see Wu et al. (1994) for additional discussion). Diameter measurements were based on the linear distance (length) determined from cursor placement as shown in the right inset of Fig. 1. Measurements showed that ghost membranes have an average diameter of about 5.7 μm. Fusion of pairs of such ghosts can lead to a spherical fusion product (e.g., see Fig. 3, *open squares* and *open diamonds*) with a diameter of about 7.5 μm. Under other conditions, a doublet is formed with a fusion zone as shown at D_{OL} or D_{FD} in Fig. 1, and diameters as shown, for example, in Figs. 3–5. Previous work (Abidor and Sowers, 1992) suggests that membrane fusion occurs within 100 ms of the application of the electric pulse. The fusion zone thus produced is called a flat diaphragm because it is visible by phase optics as an optically dense line (Chernomordik and Sowers, 1991). Generally, the length of this line increased at a high rate over the first 0.5-s interval after the pulse (Table 1). The expansion rate in the second 0.5-s interval was about 1/5 of that in the first 0.5-s interval but then fell quickly thereafter until, at about 20 s after the pulse, the rate became essentially constant (all data points were essentially on a straight line) (see Fig. 2 of Wu et al., 1994). In terms of length, the fusion zones were, depending on conditions, about 2.8–3.5 μm in diameter at 1 s after the pulse. Over the 20–120 s interval, these fusion zones increased in diameter, generally from about 3.3–3.8 μm at 20 s to 3.8–6 μm at 120 s, depending on conditions. In the 1–20 s interval, the rate of change rapidly decreased by more than an order of magnitude. Thus, the time needed for the fusion zone length to increment to the next image analysis pixel increased asymptotically (cf. representative length data in Fig. 3 with rate data in Fig. 2 of Wu et al., 1994). Thus, unlike for the 0–0.5 s interval, where the interval was short but the rate high, and for the 20–120 s interval, where the rate was low but the interval long, the manner in which the rates changed in the 1–20 s period had the effect of obscuring any condition-dependent trends. Also, no attempt was made to account in the present paper for membrane area transferred from the ghost membranes in contact to the flat diaphragm membrane area, which then internally vesiculated. However, in a previous study it was determined that 6–18% of membrane area is lost from substrate membranes as they become part of the fusion product membrane (see Chernomordik and Sowers (1991) for discussion).

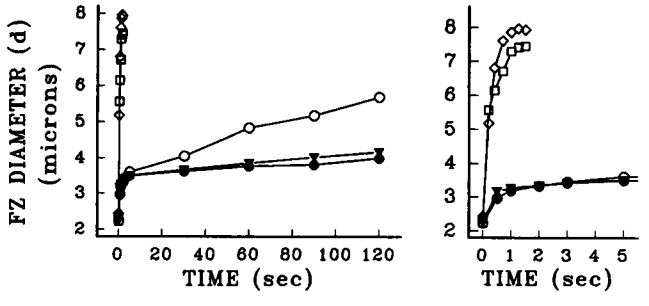

FIGURE 3 *N*-ethylmaleimide (NEM) effect on average fusion zone diameter versus time curves in fused pairs of erythrocyte ghosts. Ghost membranes in 20 mM pH 8.5 NaPi and 1 mM NEM were heat-treated and then fused. Diameter versus time plots show the entire 0–120 s period (*left*) and the 0–5 s period (*right*) after the electric pulse. All heat treatments (HT) were for 20 min. Open and solid symbols represent open lumen and flat diaphragm fusion products, respectively. ◇, NEM present and 42°C HT; □, NEM present and 39°C HT; ○, control (42°C HT but no NEM); ▼, control (NEM but no HT); ●, control (no NEM, no HT).

Experiments with heat treatments carried out while the membranes were in a different buffer

For technical reasons discussed previously (Sowers, 1993), a 20 mM pH 8.5 NaPi buffer was routinely used in this laboratory as a storage and working medium for erythrocyte ghosts and fusion experiments. For some experiments, this buffer was modified as follows.

Effects of glycerol presence or altered pH on 42°C, 20 min heat treatment at low ionic strength

Water was glycerinated before solute addition to produce final glycerol concentrations (v/v) for the buffers used for the steps as shown in Table 1, part C. The fusion zone expansion rates, flat diaphragm lifetimes, and fusion zone type were studied with a pH of 6.2 or 7.4, instead of 8.5, in both the wash and resuspension buffers (Table 1, part D).

Effect of heat treatment temperature when the heat treatment is carried out at pH 7.4 and at high ionic strength

We chose to score for ratio of open lumen fusion zones to flat diaphragm fusion zone in a much larger membrane population than we used for fusion zone expansion rate measurements (Table 1) because flat diaphragm lifetime was much more sensitive to experimental conditions than late period fusion zone expansion rates (see Table 1, parts A and B). We chose 40, 43, 46, and 49°C as heat treatment temperatures, instead of the temperatures in Table 1, Part B, because more data points would be closer together as well as inside the temperature range for the spectrin calorimetric transition. The remaining details of the experimental protocol were designed from critical information from previous studies. Ralston and Dunbar (1979) showed that spectrin had a thermotropic optical rotary dispersion transition that ranged from ~47 to 49°C at 0.1 M NaCl but from ~37 to 50°C at 0.005 M NaCl. Brandts et al. (1978) reported an analogous ionic strength dependence for the spectrin calorimetric transition, but the effect was weaker and the data were obtained over a much narrower ionic strength range. They also reported that, compared with a pH of 8.5, pHs from 8.0 to 6.5 cause an increase in the spectrin calorimetric transition by about 2–4°C (Brandts et al., 1978). Also, it has been reported that lower pHs increase the band 3-ankyrin association (Low et al., 1991). Therefore, compared with our conventional buffer, we desired to determine whether heat treatments carried out closer to a physiological pH and ionic strength would show protection against the heat treatment-induced (assumed to take place through denaturation of spectrin) destabilization of flat diaphragms. This would show up as a lower ratio of open lumens to flat diaphragms in a sample population. We thus conducted the heat treatments on membranes in pH 7.4 isotonic sodium phosphate buffer, made as previously described (Dodge et al., 1963), as well as in 20 mM pH 8.5 sodium phosphate. Also, it was necessary to move membranes from the high ionic strength buffers used for the heat treatment back to the low ionic strength needed for the fusion zone type assay. Such changes are known to reopen the hemolytic hole (Lieber and Steck, 1982a, b), which will lead to lower levels of residual hemoglobin in the experimental sample (i.e., our normal "pink" ghost preparation becomes more "white"). We have previously and rigorously determined that membrane fusion yield is highly sensitive to residual hemoglobin levels in ghost membranes (Sowers, 1990). To avoid this artifact, we conducted all heat treatments on white ghosts instead of our usual pink ghosts. We have previously shown (Sowers, 1990) that washes, by themselves, have little or no effect on membrane fusion yield. White ghosts were prepared as follows. Rabbit whole blood in Alsevers (1:1 v/v) (Wu et al., 1994) was added to 5 vol of 20 mM pH 7.4 NaPi with 0.9% NaCl (w/v). The erythrocyte pellet, from a 300 × *g* for 10 min spin, was resuspended in 20 vol of 5 mM pH 8.5 NaPi and hemolyzed for 20 mins, then spun down at 10,000 × *g* for 20 mins. This hemolysis step was repeated to hemolyze further the pink ghosts, thus ending with a white ghost pellet, which was then resuspended and washed in 20 vol of 20 mM pH 8.5 NaPi (with a high speed 10,000 × *g* for 20 min spin) into a pellet and stored overnight at 0–4°C. The next day, an aliquot of these ghost was resuspended in 20 mM pH 8.5 NaPi, and another aliquot was resuspended in isotonic pH

TABLE 1 Fusion zone (FZ): average rates of diameter increase in the early (0–0.5 s) and in the late (20–120 s) periods* after fusion, flat diaphragm lifetime‡ (in s), and FZ type§ (at 120 s), in 20 mM NaPi buffer as a function of experimental conditions (see Figs. 1 and 2 for terminology)

Factors		Rates‡ (μm/s) Early	Late	FD lifetime‡ (s)	(N)	FZ type§
A. Control, without a heat treatment (pH 8.5)¶:		1.6	.006	>120	(7)	FD
B. Experimental conditions; heat treatment (HT) with given parameters (pH 8.5)¶ :						
HT temp (°C):	*HT duration (mins):*					
39	20	1.6	.020	>120	(8)	FD
42	10	1.4	.022	65±29	(7)	OL
42	20	1.6	.017	38±24	(29)	OL
42	60	1.7	.070	7±5	(8)	OL
45, 50	20	>10	N/A	<1	(7, 7)	OL
C. Experimental conditions; steps for glycerol presence (HT = 42°C; pH 8.5)¶ :						
%	*present during*					
5	M	1.7	.016	70±16	(9)	⅓ FD
5	HT	1.7	.014	**	(8)	⅔ FD
5	HT & M	1.0	.006	>120	(9)	FD
20	HT & M	0.7	.002	>120	(7)	FD
20	HT (50°C) & M	>10	N/A	<1	(3)	OL
D. Experimental conditions; chemical treatment (see Materials and Methods) and HT for 20 mins:						
NEM (HT = 39, 42°C; pH 8.5)						
HT:						
none (control)		nd	nd	>120	(7)	FD
yes		>10	N/A	1–2	(7, 7)	OL
Diamide (HT = 39°C; pH 8.5)						
0.1 mM		1.3	nd	80±17	(9)	⅔ FD
0.5		1.7	nd	54±25	(8)	⅓ FD
2.0		1.8	nd	20±13	(7)	OL
DPG (HT = 39°C; pH 8.5)						
HT:						
none (control)		nd	nd	>120	(7)	FD
yes		nd	.010	>120	(7)	FD
WGA (HT = 42°C; pH 8.5)		nd	nd	70±38	(9)	½ FD
pH (HT = 42°C)						
7.4		nd	nd	>120	(8)	FD
6.2		nd	nd	>120	(9)	FD

N, number of measurements; FD, flat diaphragm fusion zone; OL, open lumen fusion zone; HT, heat treatment; M, measurement experiments; N/A, not applicable; nd, no difference (averages of one group well within standard deviation bars of other group) from respective conditions listed under Part A or B; ** not done because of very small sample population.

* Average rate measurements at 20–22°C were from all *N* members in a group regardless of whether the flat diaphragm broke down into an open lumen before the end of the 120 s period (SD) for any average in one group ranged ±4–22% of the value for that average (see also Wu et al., 1994).

‡ Average flat diaphragm lifetimes (+/− SD) are from only those flat diaphragms that broke down into open lumens before the end of the 120 s observation period. Flat diaphragm lifetimes >120 s were generally stable for up to days after induction (see Wu et al., 1994).

§ Fusion zone type at the end of the 120 s observation period. OL or FD if one type is predominant (i.e., ≥80–90% of all FZs), or given as or nearest approximate fraction.

¶ From Wu et al. (1994).

7.4 NaPi. After standing on ice for 2 h, each aliquot was heat-treated, spun down, resuspended in 40 vol of 20 mM pH 8.5 NaPi, and left on ice for 25 min, and then spun into pellets for storage until the fusion assay was conducted. Fusion zones were induced between pairs of erythrocyte ghosts, as above, and then visually inspected at 2–6 min after the electric pulse to determine whether they had an open lumen or a flat diaphragm. The percentage of all fusion zones that were open lumens was calculated from these counts using the formula $(OL/(OL + FD)) \times 100$. Sample populations of fusion zones scored under any given experimental condition contained $132 < N < 496$ fusion zones.

Erythrocyte ghost prefusion chemical treatments at low ionic strength and pH 8.5

Chemical species were present in the wash and/or the resuspension buffers under the following conditions before or without a heat treatment and the microscopy (Table 1, Part D). *N*-ethylmaleimide (NEM): ghost membranes were incubated for 30 min at 0°C in the wash buffer with NEM present at 1 mM. NEM was also present at this concentration in the resuspension buffer. Diamide: only the resuspension buffer contained diamide, at the concentrations given in Table 1. Suspensions of ghost membrane were incubated in this buffer for 60 min at 0°C. 2,3-diphosphoglycerate (DPG): DPG (also known as 2,3-bisphosphoglycerate, or BPG) was present at 5 mM in the wash buffer (during the 10-min centrifugation) but not in the resuspension buffer. This allowed minute amounts of DPG to enter the cytoplasmic compartment before the hemolytic hole resealed. Wheat germ agglutinin (WGA): ghost membranes were incubated for 30 min at 0°C with WGA present at 2 μg/ml in both the wash buffer and the resuspension buffer and then heat-treated (42°C) or not heat-treated before making the measurements.

The heat treatments were carried out at both 39 and 42°C when the ghosts were exposed to *N*-ethylmaleimide (NEM), but only 39°C for diamide and 2,3-diphosphoglycerate (DPG) because it has been reported (Streichman et al., 1988; Shaklai et al., 1978; Sheetz and Casaly, 1980; Moriyama et al., 1993; Schindler et al., 1980; Lelkes and Fodor, 1991) that exposure to these molecular species either weakens the spectrin-spectrin-associated protein

binding or lowers the onset temperature for heat treatment effects. We thus expected that heat treatment effects on the diameter versus time curves might similarly occur at a lower heat-treatment temperature. NEM-treated ghosts became more cup-shaped and then, upon heat treatment, slightly smaller and spherical. The exposure to DPG in the wash buffer caused a substantial fraction of all ghosts to shape change from spherocytes to stomatocytes. Heat treating the DPG-exposed ghosts converted them back to spherocytes. WGA had no perceptible effect on ghost shape. In all cases, membrane fusion yields were not significantly affected by these chemical treatments.

RESULTS AND DISCUSSION

Overview

An earlier study from this laboratory (Wu et al., 1994) showed that fusion zone diameter versus time curves in fused pairs of erythrocyte ghosts typically have a condition-dependent kinetic expansion signature with a rapid expansion in an *early* and short (0–0.5 s after the pulse) period and a slow and essentially linear expansion over a *late* and long (20–120 s after the pulse) period. The same study showed that over an *intermediate* (0.5–1.0 to 20 s) period, the diameter expansion rate undergoes a more than 1.5 order of magnitude decrease with a dependence on time that cannot be determined with high resolution because of present limitations in instrument spatial resolution (see Fig. 2 of Wu et al., 1994). Also, the 0.5–1.0 s and the 20 s borders of this period are somewhat uncertain for the same reason (see additional discussion under Materials and Methods). In view of the uncertainty in the quantitative data from the *intermediate* period, discussion of the fusion zone diameter expansion curve in the present study will therefore be limited to the rates in only the *early* and *late* periods. Another observable parameter that was identified in the previous study is flat diaphragm lifetime (cf. Figs. 1 and 2). The purpose of the present study was to characterize the sensitivity of both the expansion signature and the flat diaphragm lifetime to chemical conditions in the buffer and to molecular species known to react with one or more components of the membrane skeleton.

Table 1 shows results of the present study and, for comparison, relevant results of our previous study (Wu et al., 1994). The new data from the present study include fusion zone expansion rates for conditions involving exposures to NEM, diamide, DPG, WGA, and experiments conducted at low pH in both a low and a high ionic strength buffer. Flat diaphragm lifetimes for these conditions and predominant fusion zone *type* in the fusion product populations are also new and given for all of these experimental conditions (Table 1, Parts A–C). Complete diameter versus time curves for the experimental conditions involving exposure to NEM, diamide, and 2,3-DPG are relevant and shown in Figs. 3, 4, and 5. Fig. 6 shows the effect of heat treatment *temperature* on the ratio of open lumen fusion zones to flat diaphragm fusion zones in 20 mM pH 8.5 NaPi buffer versus isotonic pH 7.4 NaPi buffer.

Heat treatments (Table 1, Part B) caused the average fusion zone expansion rates in the early period to be in the 1.4–1.7 μm/s range, which is similar to 1.6 μm/s found under

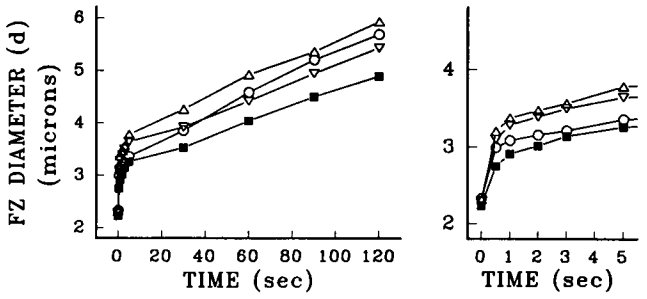

FIGURE 4 Diamide effect on average fusion zone diameter versus time curves in fused pairs of erythrocyte ghosts. Ghosts in diamide at the following concentrations were heat-treated at 39°C and then fused: ■, 0 mM (control); ○, 0.1 mM; ▽, 0.5 mM; △, 2.0 mM. Note that the fraction of all flat diaphragms that became open lumens increased with diamide concentration (cf. Table 1). All other parameters are as in Fig. 3.

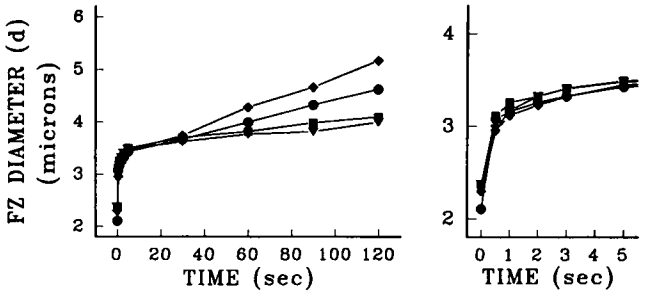

FIGURE 5 2,3-diphosphoglyceric acid (DPG) effect on average fusion zone diamter versus time curves in fused pairs of erythrocyte ghosts. Ghosts in DPG at 5 mM were then washed free of the DPG before the 39°C HT and then were fused: ●, DPG present then washed out before HT; ■, control (DPG present then washed out but no HT); ▼, control (no DPG, no HT); ◆, control (HT but no DPG). Note that none of the flat diaphragms broke down into open lumens by the end of the observation period. All other parameters are as in Fig. 3.

the control conditions (Table 1, Part A), and to increase slightly with the duration of the 42°C heat treatment. In the late period, the diameter increased with time in a very slow (0.006 μm/s) but essentially linear manner. However, heat treatments of 39°C, 20 min, and 42°C for 10–20 min increased the late period rate of expansion by a factor of three over controls, and a heat treatment of 42°C for 60 min increased this rate by an additional factor of three over the 20 min heat treatment. A heat treatment at 45 or 50°C caused the fusion zone diameter to expand to a complete sphere in 1–2 s without producing a flat diaphragm. Flat diaphragms usually broke down into open lumens for any heat treatment ≥42°C, but average flat diaphragm lifetime went down by a factor of 10 for an increase in the 42°C heat treatment duration from 10 to 60 min (Table 1, Part B). The fact that spectrin, and only spectrin, in the erythrocyte ghost membrane has a calorimetric transition in this temperature range (Brandts et al., 1977; Ralston and Dunbar, 1979) and our finding that the presence of glycerol protects against this heat treatment effect on fusion zone expansion led us to hypothesize that the membrane skeleton played a major role in con-

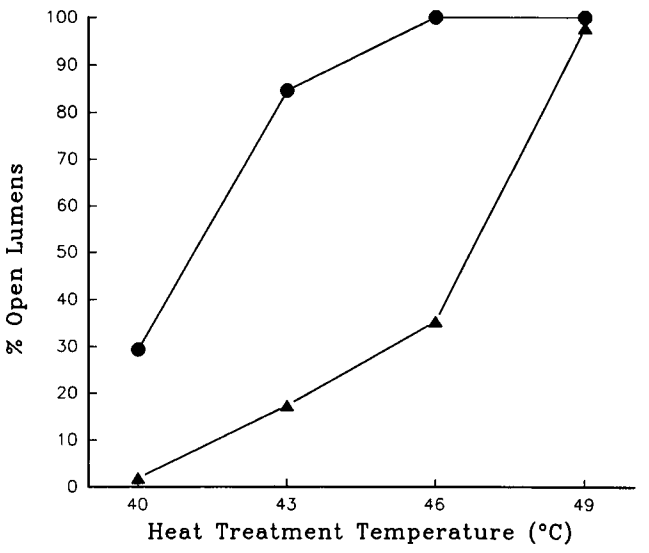

FIGURE 6 Fraction (as a percentage) of all flat diaphragm fusion zones that break down into open lumens after white ghost membranes receive a heat treatment, at the given temperature, in 20 mM pH 8.5 sodium phosphate (●) or isotonic pH 7.4 sodium phosphate (▲) and are then aligned into contact and fused. Fusion zone type was scored only from fused pairs of ghosts and not from fusions involving pearl chains containing three or more ghosts. Number (N) of fused pairs in population for each point was $132 < N < 496$.

trolling both the fusion zone expansion and the flat diaphragm lifetime (Wu et al., 1994).

Although the presence of 5% (v/v) glycerol during measurements (Table 1, Part C) had little effect on expansion rates, it did prevent the breakdown of about ⅓ of the flat diaphragms even though the remainder broke down after about the same lifetime (70 vs. 65 s). Glycerol present at 5% during the heat treatment instead of during the expansion measurements still had no effect on the rates but prevented ⅔, or twice as many, of the flat diaphragms from breaking down. Glycerol present at 5% during both the heat treatment and the expansion measurements caused a significant decrease in expansion rates in both the early and late periods and prevented all flat diaphragms from breaking down. At 20% glycerol, both expansion rates were significantly decreased. This showed that the presence of glycerol had effects in addition to elevation of the denaturation temperature for spectrin (see Wu et al. (1994) for discussion). Although the viscosity of an aqueous solution at 20% glycerol is double that of pure water, a heat treatment at 50 instead of 42°C caused the fusion zones to expand at the maximum rate (>10 μm/s), showing that, in addition to the heat-sensitive membrane skeleton, the aqueous viscosity, hydration, and membrane permeability were not limiting or controlling any of the expansion rates.

Effects of membrane skeleton agents

Our efforts to gain additional information about the involvement of the membrane skeleton in the fusion zone diameter expansion curves and flat diaphragm stability were aided by previous studies that showed that spectrin-related erythrocyte membrane properties had specific sensitivities to chemical modification or exposure to biologically relevant molecular species that had binding sites primarily on spectrin or other membrane skeleton components. NEM, diamide, and DPG are known to bind to spectrin in higher numbers per molecule than to any other membrane component (Fischer et al., 1978; Haest et al., 1978; Becker et al, 1986; Streichman et al., 1988). Electron microscopy shows diamide-bound spectrin molecules as having a ringlike instead of a linear rod-like conformation (Fischer et al., 1978; Haest et al., 1979; Becker et al., 1986). Also, it is known that exposure to these molecular species will i) lower the onset temperature for thermally induced dissociation of spectrin network components (Streichman et al., 1988; Smith and Palek, 1980), ii) affect the membrane deformability and stability of erythrocytes as measured by ektacytometry (Chasis and Mohandas, 1986), iii) weaken the spectrin-skeleton protein complexes based on the dissociation of protein complexes (Sheetz and Casaly, 1980), or iv) increase integral protein lateral mobility (Schindler et al., 1980). Finally, wheat germ agglutinin (WGA) is known to i) enhance binding of spectrin to glycophorin in the plasma membrane (Chasis et al., 1985; Chasis and Schrier, 1989), ii) inhibit temperature-induced and pH-induced vesiculation (Lelkes and Fodor, 1991), and iii) block shape changes from occurring (Lovrien and Anderson, 1980).

Results of our experiments (Fig. 3 and Table 1, part D) show that NEM exposure followed by either a 39 or 42°C heat treatment led to fusion products that became spheres within 1–2 s (i.e., had a dramatically higher rate of fusion zone diameter expansion). Also, diamide exposure followed by a 39°C heat treatment led to a progressive, concentration-dependent increase in rate of fusion zone diameter expansion in the first 0–1 s interval after the pulse, and a large reduction in the flat diaphragm lifetime for those fusions that ended in open lumens (Fig. 4). Moreover, exposure of ghost membranes to DPG followed by a 39°C heat treatment diminished the rate in the 20–120 s interval to one-half of the rate for the heat treatment without DPG exposure (Fig. 5 and Table 1, Part D).

Although WGA had essentially no effect on either the fusion zone expansion kinetics or the average lifetime for those flat diaphragms that broke down, it did prevent about half of the flat diaphragms from breaking down into open lumens (Table 1, Part D). Our results are consistent with an explanation based on WGA-enhanced spectrin-glycophorin binding, because other work (Chasis and Schrier, 1989) implied that binding of WGA to an erythrocyte surface is not likely to cause extracellular cross-linking or lattice formation.

pH and ionic strength effects

Our observation that a pH of 6.2 or 7.4, instead of 8.5, in the 20 mM NaPi buffer during the heat treatment would *block* (Table 1, Part D) the heat treatment-induced destabilization

of the flat diaphragm is consistent with reports that, compared with a pH of 8.5, pHs from 8.0 to 6.5 cause an increase in the spectrin calorimetric transition by about 2–4°C (Brandts et al., 1978). Also, compared with a pH of 8.5 at low ionic strength, it was found (Fig. 6) that a pH of 7.4 and high ionic strength dramatically shifted upward, by about 5°C, the temperature needed to induce flat diaphragm breakdown into open lumens. Also, this finding is consistent with a report that lower pHs increase the band 3-ankyrin association (Low et al., 1991).

Rounding up rates in fused mitochondrial inner membranes, a membrane system without a membrane skeleton

Mitochondrial inner membranes (1–1.5 μm diameter) do not contain a known membrane skeleton. Although fusion yields have not been quantitatively characterized in this membrane, we qualitatively estimate that in our experiments about half of the membranes in pearl chains undergo the observed rounding up after the application of the fusogenic electric pulse, and the other half of the membranes remain unfused and separate by Brownian motion if the alternating electric field is turned off after the pulse. In contrast to the rounding up in fused erythrocyte membranes, which takes place over a time scale of minutes, we found that the electrofusion of mitochondrial inner membranes always led to a rapid expansion of fused doublets into single large spheres in 0.5–1 s. This result is consistent with the time scales needed for fusion zone expansions (to final forms, which are spherical) reported from other laboratories for other membrane skeleton-free membrane-cell systems. For example, the post-fusion swelling step in electrofused bacterial spherocytes (which are spectrin free and have no cell wall) is rapid, taking place within 1 s (Ruthe and Adler, 1985). In contrast, cell fusion induced between spectrin-containing erythrocytes and nucleated cells by a virus (Sarkar et al., 1989) or between two cultured myeloma cells by a laser light pulse (Steubing et al., 1991) is, in both cases, slow and on the order of several minutes (i.e., the same time scale as in our data shown in Fig. 3).

Mechanistic implications

Our data show that the rates in fusion zone expansion curves and the flat diaphragm lifetime can be highly condition-dependent and vary by a factor of 3–10 or more. Also, these two dependent variables can respond differently to a given experimental condition. The effect of the presence of biologically relevant molecular species known to react primarily with or bind to membrane skeleton proteins further supports our hypothesis that the membrane skeleton is a major source of mechanical influence on the rounding up process and that this influence has the effect of *limiting* the rate of the rounding up process. Our observation that WGA stabilizes flat diaphragms and DPG alters late phase expansion rates invites the speculation that the influence of the membrane skeleton on plasma membrane mechanical properties could be under biological control. This is consistent with some previous reports. For example, the cell rounding, which is associated with cells entering mitosis rather than cell fusion, is correlated with the relocation of spectrin in cells (Fowler and Adam, 1992). Also, experimentally induced cell activation leads to membrane-skeleton reorganization (Bretscher, 1989; Perrin et al., 1992; Lee et al., 1988). Considering that spectrin and at least some spectrin-associated proteins have binding sites for divalent cations, kinases, and proteins known or believed to have regulatory roles (see Bennett, 1990), it is possible that the membrane skeleton may function as more than just a passive scaffold with fixed mechanical properties.

An unanswered question is how much of a contribution to the effects we observed come from alterations in the lipid component (e.g., asymmetry, protein-lipid ratio, chemical changes, area per headgroup). A reasonable amount of experimental (Kas and Sackmann, 1991; Farge and Devaux, 1992) and theoretical (Svetina and Zeks, 1989) work has already been published on a shape transformation problem in vesicles and pure lipid systems that can be, in principal, used as a guide to design relevant experiments using a biomembrane containing a membrane skeleton. The availability of protocols to further manipulate erythrocyte plasma membrane (Vertessy and Steck, 1989; for reviews, see Leonards and Ohki, 1983; Beaudoin and Grondin, 1991) suggest future possible work. Another unanswered question is how much contribution to the effects come from native conformation versus partly or completely heat-denatured subpopulations of spectrin molecules. Effects that we are observing from DPG could be through occupancy of sites on native or partly denatured spectrin or both. We used 42°C, 20 min heat-treated membranes extensively in this and our earlier study (Wu et al., 1994) to take advantage of its relatively high specificity; its major effect has been shown to be on spectrin and only spectrin (Brandts et al., 1978). Also, the heat treatment we used makes late period fusion zone expansion rates higher and therefore easier to measure and causes flat diaphragm lifetime to be short enough to make it practicable to characterize its dependence on experimental conditions. This heat treatment was targeted to roughly the midpoint of (rather than completely through) the spectrin calorimetric transition with the idea of *retaining* a substantial amount of spectrin in the native conformation. In future studies, especially in non-heat-treated membranes, the eventual analysis of the overall fusion process in terms of force components and mechanical properties will likely reveal more about the structure-function relationships in the membrane skeleton and how they are biologically regulated.

This work was supported by Office of Naval Research grant N00014–92-J-1053 to A. E. Sowers.

REFERENCES

Abidor, I. G., and A. E. Sowers. 1992. Kinetics and mechanism of cell membrane electrofusion. *Biophys. J.* 60:1557–1569.

Beaudoin, A. R., and G. Grondin. 1991. Shedding of vesicular material from the cell surface of eukaryotic cells: different cellular phenomena. *Biochim. Biophys. Acta.* 1071:203–219.

Becker, P. S., C. M. Cohen, and S. E. Lux. 1986. The effect of mild diamide oxidation on the structure and function of human erythrocyte spectrin. *J. Biol. Chem.* 261:4620–4628.

Bennett, V. 1990. Spectrin-based membrane skeleton: a multipotential adaptor between plasma membrane and cytoplasm. *Physiol. Rev.* 70:1029–1065.

Bessis, M. 1973. Living blood cells and their ultrastructure. Springer Verlag, New York. 767 pp.

Boss, W. F. 1987. Fusion-permissive protoplasts: a plant system for studying cell fusion. *In* Cell Fusion. A. E. Sowers, editor. Plenum Press, New York. 145–166.

Brandts, J. F., L. Erickson, K. Lysko, A. T. Schwartz, and R. D. Taverna. 1977. Calorimetric studies of the structural transitions of the human erythrocyte membrane. The involvement of spectrin in the A transition. *Biochemistry.* 16:3450–3454.

Brandts, J. F., R. D. Taverna, E. Sadasivan, and K. A. Lysko. 1978. Calorimetric studies of the structural transitions of the human erythrocyte membrane: studies of the B and C transitions. *Biochim. Biophys. Acta.* 512:566–578.

Branton, D., C. Cohen, and J. Tyler. 1981. Interaction of cytoskeletal proteins on the human erythrocyte membrane. *Cell.* 24:24–32.

Bretscher, A. 1989. Rapid phosphorylation and reorganization of ezrin and spectrin accompany morphological changes induced in A-431 cells by epidermal growth factor. *J. Cell Biol.* 108:921–930.

Byers, T. J., and D. Branton. 1985. Visualization of the protein associations in the erythrocyte membrane skeleton. *Proc. Natl. Acad. Sci. USA.* 82: 6153–6157.

Chasis, J. A., and N. Mohandas. 1986. Erythrocyte membrane deformability and stability: two distinct membrane properties that are independently regulated by skeletal protein associations. *J. Cell Biol.* 103:343–350.

Chasis, J. A., N. Mohandas, and S. B. Shohet. 1985. Erythrocyte membrane rigidity induced by glycophorin A-ligand interaction. Evidence for a ligand-induced association between glycophorin A and skeletal proteins. *J. Clin. Invest.* 75:1919–1926.

Chasis, J. A., and S. L. Schrier. 1989. Membrane deformability and the capacity for shape change in the erythrocyte. *Blood.* 7:2562–2568.

Chernomordik, L. V., and A. E. Sowers. 1991. Evidence that the spectrin network and a nonosmotic force control the fusion product morphology in electrofused erythrocyte ghosts. *Biophys. J.* 60:1026–1037.

Deuticke, B. 1968. Transformation and restoration of biconcave shape of human erythrocytes induced by amphiphilic agents and changes of ionic environment. *Biochim. Biophys. Acta.* 163:494–500.

Dodge, J. T., C. Mitchell, D. J. Hanahan. 1963. The preparation and chemical characterization of hemoglobin-free ghosts of human erythrocytes. *Arch. Biochem. Biophys.* 100:119–130.

Duzgunes, N., editor. 1993a. Membrane Fusion Techniques, Part A. *Methods Enzymol.* 220:1–443.

Duzgunes, N., editor. 1993b. Membrane Fusion Techniques, Part B. *Methods Enzymol.* 221:1–462.

Elgsaeter, A., B. T. Stokke, A. Mikkelsen, and D. Branton. 1986. The molecular basis of erythrocyte shape. *Science.* 234:1217–1223.

Evans, E. A. 1989. Structure and deformation properties of red blood cells: concepts and quantitative methods. *Methods Enzymol.* 173:3–35.

Farge, E., and P. F. Devaux. 1992. Shape changes of giant liposomes induced by an asymmetric transmembrane distribution of phospholipids. *Biophys. J.* 61:347–357.

Fischer, T. M., C. W. M. Haest, M. Stohr, D. Kamp, and B. Deuticke. 1978. Selective alteration of erythrocyte deformability by SH-reagents. Evidence for an involvement of spectrin in membrane shear elasticity. *Biochim. Biophys. Acta.* 510:270–282.

Fowler, V. M., and E. J. H. Adam. 1992. Spectrin redistributes to the cytosol and is phosphorylated during mitosis in cultured cells. *J. Cell Biol.* 119: 1559–1572.

Grimaila, R. J., B. A. Fuller, P. D. Rennert, M. B. Nelso, M.-L. Hammarksjold, B. Potts, M. Murray, S. D. Putney, and G. Gray. 1992. Mutations in the principal neutralization determinant of human immunodeficiency virus type 1 affect syncytium formation, virus infectivity, growth kinetics, and neutralization. *J. Virol.* 66:1875–1883.

Gross, D., L. M. Loew, and W. W. Webb. 1986. Optical imaging of cel membrane potential changes induced by applied electric fields. *Biophys. J.* 50:339–348.

Haest, C. W. M., G. Plasa, D. Kamp, and B. Deuticke. 1978. Spectrin as a stabilizer of the phospholipid asymmetry in the human erythrocyte membrane. *Biochim. Biophys. Acta.* 509:21–32.

Harris, H. 1970. Cell Fusion. Harvard University Press, Cambridge, MA. 108 pp.

Harvey, E. N. 1954. Tension at the cell surface. *Protoplasmatologia.* 2:1–30.

Horvath, C. M., R. G. Paterson, M. A. Shaughnessy, R. Wood, and R. A. Lamb. 1992. Biological activity of paramyxomirus fusion proteins: factors influencing formation of syncytia. *J. Virol.* 66:4564–4569.

Kas, J., and E. Sackmann. 1991. Shape transitions and shape stability of giant phospholipid vesicles in pure water by area-to-volume changes. *Biophys. J.* 60:825–844.

Knutton, S. 1977. Studies of membrane fusion. II. fusion of human erythrocytes by sendai virus. *J. Cell Sci.* 28:189–210.

Lee, J. K., J. D. Black, E. A. Repasky, R. T. Kubo, and R. B. Bankert. 1988. Activation induces a rapid reorganization of spectrin in lymphocytes. *Cell.* 55:807–816.

Lelkes, G., and I. Fodor. 1991. Formation of large, membrane skeleton-free erythrocyte vesicles as a function of the intracellular pH and temperature. *Biochim. Biophys. Acta.* 1065:135–144.

Leonards, K., and S. Ohki. 1983. Isolation and characterization of large (0.5–1 um) cytoskeleton-free vesicles from human and rabbit erythrocytes. *Biochim. Biophys. Acta.* 728:383–393.

Lew, V. L., A. Hockaday, C. J. Freeman, and R. M. Bookchin. 1988. Mechanism of spontaneous inside-out vesiculation of red cell membranes. *J. Cell Biol.* 106:1893–1901.

Lieber, M. R., and T. L. Steck. 1982a. A description of the holes in human erythrocyte membrane ghosts. *J. Biol. Chem.* 257:11651–11659.

Lieber, M. R., and T. L. Steck. 1982b. Dynamics of the holes in human erythrocyte membrane ghosts. *J. Biol. Chem.* 257:11660–11666.

Lovrien, R. E., and R. A. Anderson. 1980. Stoichiometry of wheat germ agglutinin as a morphology controlling agent and as a morphology protective agent for the human erythrocyte. *J. Cell Biol.* 85:534–548.

Low, P. S., B. M. Willardson, N. Mohandas, M. Rossi, and S. Shohet. 1991. Contribution of the band 3-ankyrin interaction to erythrocyte membrane mechanical stability. *Blood.* 77:1581–1586.

Lucy, J. A. 1978. Mechanisms of chemically induced cell fusion. *In* Cell Surface Reviews, Vol. 5. Membrane Fusion. G. Poste, and G. L. Nicolson, editors. North-Holland, Amsterdam. 268–304.

McGough, A. M., and R. Josephs. 1990. On the structure of erythrocyte spectrin in partially expanded membrane skeletons. *Proc. Natl. Acad. Sci. USA.* 87:5208–5212.

Monck, J. R., G. Alvarez de Toledo, and J. M. Fernandez. 1990. Tension in secretory granule membranes causes extensive membrane transfer through the exocytotic fusion pore. *Proc. Natl. Acad Sci. USA.* 87: 7804–7808.

Monck, J. R., A. F. Oberhauser, G. Alvarez de Toledo, and J. M. Fernandez. 1991. Is swelling of the secretory granule matrix the force that dilates the exocytotic fusion pore? *Biophys. J.* 59:39–47.

Moriyama, R., C. R. Lombardo, R. F. Workman, and P. S. Low. 1993. Regulation of linkages between the erythrocyte membrane and its skeleton by 2,3-diphosphoglycerate. *J. Biol. Chem.* 268:10990–10996.

Oberhauser, A. R., J. R. Monck, and J. M. Fernandez. 1992. Events leading to the opening and closing of the exocytotic fusion pore have markedly different temperature dependencies: kinetic analysis of single fusion events in patch-clamped mouse mast cells. *Biophys. J.* 61:800–809.

Palek, J., and S. E. Lux. 1983. Rec cell membrane skeletal defects in hereditary and acquired hemolytic anemias. *Sem. Hematol.* 20:189–224.

Perrin, D., D. Moller, K. Hanke, and H.-D. Soling. 1992. cAMP and Ca^{++}-mediated secretion in parotid acinar cells is associated with reversible changes in the organization of the cytoskeleton. *J. Cell Biol.* 116: 127–134.

Pinto da Silva, P., K. Shimizu, and C. Parkison. 1980. Fusion of human erythrocytes induced by sendai virus: freeze-fracture aspects. *J. Cell Sci.* 43:419–432.

Pohl, H. A. 1978. *Dielectrophoresis.* Cambridge University Press, London. 579 pp.

Poste, G., and G. L. Nicolson, editors. 1978. Cell Surface Reviews, Vol. 5. Membrane Fusion. Elsevier/North Holland Biomedical Press, New York. 862 pp.

Ralston, G. B., and J. C. Dunbar. 1979. Salt and temperature-dependent conformation changes in spectrin from human erythrocyte membranes. *Biochim. Biophys. Acta.* 579:20–30.

Ringertz, N. R., and R. E. Savage. 1976. Cell Hybrids. Academic Press, New York. 366 pp.

Roizman, B. 1962. Polykaryocytosis. *Cold Spring Harbor Symp. Quant. Biol.* 27:327–342.

Ruthe, H.-J., and J. Adler. 1985. Fusion of bacterial spheroplasts by electric fields. *Biochim. Biophys. Acta.* 819:105–113.

Sarkar, D. P., S. J. Morris, O. Eidelman, J. Zimmerberg, and R. Blumenthal. 1989. Initial stages of influenza hemagglutinin-induced cell fusion monitored simultaneously by two fluorescent events: cytoplasmic continuity and lipid mixing. *J. Cell Biol.* 109:113–122.

Schierenberg, E. 1987. Laser-induced cell fusion. *In* Cell Fusion. A. E. Sowers, editor. Plenum Press, New York. 409–418.

Schindler, M., D. E. Koppel, and M. P. Sheetz. 1980. Modulation of membrane protein lateral mobility by polyphosphates and polyamines. *Proc. Natl. Acad. Sci. USA.* 77:1457–1461.

Senda, M., J. Takeda, S. Abe, and T. Nakamura. 1979. Induction of cell fusion of plant protoplasts by electrical stimulation. *Plant Cell Physiol.* 20:1441–1443.

Shaklai, N., L. Benitez, and H. M. Ranney. 1978. Binding of 2,3-diphosphoglycerate by spectrin and its effect on oxygen affinity of hemoglobin. *Am. J. Physiol.* 234:C36–C40.

Sheetz, M. P., and J. Casaly. 1980. 2,3-Diphosphoglycerate and ATP dissociate erythrocyte membrane skeletons. *J. Biol. Chem.* 255:9955–9960.

Sheetz, M. P., and S. J. Singer. 1974. Biological membranes as bilayer couples: a molecular mechanism of drug-erythrocyte interactions. *Proc. Natl. Acad. Sci. USA.* 71:4457–4461.

Smith, D. K., and J. Palek. 1983. Sulfhydryl reagents induce altered spectrin self-association, skeletal instability, and increased thermal sensitivity of red cells. *Blood.* 6:1190–1196.

Sowers, A. E. 1983. Fusion of mitochondrial inner membranes by electric fields produces inside-out vesicles: visualization by freeze-fracture electron microscopy. *Biochim. Biophys. Acta.* 735:426–428.

Sowers, A. E. 1990. Low concentrations of macromolecular solutes significantly affect electrofusion yield in erythrocyte ghosts. *Biochim. Biophys. Acta.* 1025:247–251.

Sowers, A. E. 1993. Membrane electrofusion: a paradigm for study of membrane fusion mechanisms. *Methods Enzymol.* 220:196–210.

Sowers, A. E., and C. R. Hackenbrock. 1981. Rates of lateral diffusion of intramembrane particles: measurement by electrophoretic displacement and rerandomization. *Proc. Natl. Acad. Sci. USA.* 78:6246–6250.

Sowers, A. E., and V. Kapoor. 1988. The mechanism of erythrocyte ghost fusion by electric field pulses. *In* Proceedings of the International Symposium on Molecular Mechanism of Membrane Fusion. S. Ohki, D. Doyle, T. D. Flanagan, S.-W. Hui, and E. Mayhew, editors. Plenum Press, New York. 237–254.

Steubing, R. W., S. Cheng, W. H. Wright, Y. Numajiri, and M. W. Berns. 1991. Laser induced cell fusion in combination with optical tweezers: the laser cell fusion trap. *Cytometry.* 12:505–510.

Streichman, S., E. Hertz, and I. Tatarsky. 1988. Direct involvement of spectrin thiols in maintaining erythrocyte membrane thermal stability and spectrin dimer self-association. *Biochim. Biophys. Acta.* 942:333–340.

Svetina, S., and B. Zeks. 1989. Membrane bending energy and shape determination of phospholipid vesicles and red blood cells. *Eur. Biophys. J.* 17:101–111.

Ursitti, J. A., and J. B. Wade. 1993. Ultrastructure and immunocytochemistry of the isolated human erythrocyte membrane skeleton. *Cell Motil. Cytoskel.* 25:30–42.

Vertessy, G. G., and T. L. Steck. 1989. Elasticity of the human red cell membrane skeleton. Effects of temperature and denaturants. *Biophys. J.* 55:255–262.

Waugh, R. E., and P. Agre. 1988. Reductions of erythrocyte membrane viscoelastic coefficients reflect spectrin deficiencies in hereditary spherocytosis. *J. Clin. Invest.* 81:133–141.

White, J. 1992. Membrane fusion. *Science.* 258:917–924.

Wojcieszyn, J. W., R. A. Schlegel, K. Lumley-Sapanski, and K. A. Jacobson. 1983. Studies on the mechanism of polyethylene glycol-mediated cell fusion using fluorescent membrane and cytoplasmic probes. *J. Cell Biol.* 96:151–159.

Wu, Y.-K., R. A. Sjodin, and A. E. Sowers. 1994. Distinct mechanical relaxation components in pairs of erythrocyte ghosts undergoing fusion. *Biophys. J.* 66:114–119.